arXiv:nlin/0105013v1 [nlin.CD] 8 May 2001

Critical States and Fractal Attractors in Fractal Tongues: Localization in the Harper map

Surendra Singh Negi and Ramakrishna Ramaswamy

School of Physical Sciences

Jawaharlal Nehru University, New Delhi 110 067, INDIA

(February 8, 2008)

Abstract

Localized states of Harper's equation correspond to strange nonchaotic attractors (SNAs) in the related Harper mapping. In parameter space, these fractal attractors with nonpositive Lyapunov exponents occur in fractally organized tongue–like regions which emanate from the Cantor set of eigenvalues on the critical line $\epsilon = 1$. A topological invariant characterizes wavefunctions corresponding to energies in the gaps in the spectrum. This permits a unique integer labeling of the gaps and also determines their scaling properties as a function of potential strength.

Typeset using REVTEX

The Harper equation [1],

$$\psi_{n+1} + \psi_{n-1} + V(n)\psi_n = E\psi_n, \tag{1}$$

where ψ_n denotes the wave-function at lattice site n, and $V(n) = 2\epsilon \cos 2\pi(n\omega+\phi_0)$ with ω irrational has been extensively studied in the context of localization. This discrete Schrödinger equation for a particle in a quasiperiodic potential on a lattice, arises in a number of different problems [2–4]. It is known [5] that the eigenstates can be extended ($\epsilon < 1$), localized ($\epsilon > 1$), or critical ($\epsilon = 1 \equiv \epsilon_c$), when the eigenvalue spectrum is singular–continuous [6], and the states are power–law localized [7,8]. Renormalization group studies [9–11] of this model have been very effective in establishing the multifractal nature of the wavefunctions of such states and of the eigenvalue spectrum [12].

On transforming to Ricatti variables [13] $\psi_{n-1}/\psi_n \to x_n$, Eq. (1) reduces to the (equivalent) Harper map [14],

$$x_{n+1} = -[x_n - E + 2\epsilon \cos 2\pi\phi_n]^{-1} \tag{2}$$

$$\phi_{n+1} = \{\omega + \phi_n\} \tag{3}$$

where $\{y\} \equiv y \bmod 1$. Viewed as a skew–product dynamical system, this is now a driven mapping of the infinite strip $(\infty, \infty) \otimes [0, 1]$ to itself. Irrational ω implies that the forcing in Eq. (2) is quasiperiodic, the lattice site index n in the quantum problem becoming the iteration or time index in the map.

The Harper map, which we study in this Letter, provides an alternate means of analyzing the eigenvalue spectrum of the Harper equation. Boundary conditions that must be imposed on Eq. (1) in order to determine eigenstates become conditions on the dynamical states in the map, Eqs. (2-3), where E now appears as a parameter. Note that since the map is reversible, there is no chaotic motion, and furthermore, because the driving is quasiperiodic, there are also no periodic orbits. For large enough ϵ, the attractor of the dynamics is a fractal, and on this attractor, the dynamics is nonchaotic [14,15]: these are therefore strange nonchaotic

attractors (SNAs) [16] which are generic in quasiperiodically forced systems. In addition there can be a variety of other nonfractal quasiperiodic (torus) attractors.

When E is an eigenvalue, a correspondence relates localized states of the quantum problem to SNAs in the associated map. This equivalence that was first noted by by Bondeson, Ott and Antonsen [17] in a study of the continuous version of the same problem. The wavefunctions for critical and extended states have a quasiperiodic symmetry [15], while the fractal fluctuations of the amplitudes of the localized states [11] appear as fractal density fluctuations in the attractors of the map. The nontrivial Lyapunov exponent of the system is given by

$$\lambda = \lim_{N\to\infty} \frac{1}{N} \sum_{i=1}^{N} y_n, \tag{4}$$

where $y_n = \ln x_{n+1}^2$, the so–called stretch exponent, is the derivative of the mapping, Eq. (2). At ϵ_c, if E is an eigenvalue of the quantum problem, then this quantity is exactly zero [15]; see Fig. 1. Above ϵ_c, the localization length for quantum states, γ, is inversely related to the Lyapunov exponent [5], $\lambda^{-1} = -\gamma/2$. Knowledge of this equivalence thus permits the complete determination of the quantum spectrum of the Harper system through a study of the Lyapunov exponents of the Harper map. At every eigenvalue (Fig. 1) there is a bifurcation from a quasiperiodic attractor to a SNA, when the Lyapunov exponent becomes zero [18].

The spectrum of the Harper equation is invariant under the transformation $\omega \to 1-\omega$, and is symmetric about $E = 0$, so it suffices to consider only positive eigenvalues and $\omega > 1/2$. The behaviour of the spectral *gaps* has been of considerable interest [4], and we study this here by describing the phase–diagram of this system for $\omega_{\rm g} = (\sqrt{5}-1)/2$, the inverse golden–mean ratio.

At $\epsilon = 0$, the states of the quantum system form a band between energies $0 \le E \le 2$. As ϵ is increased, the gaps open up and merge as $\epsilon \to \epsilon_c$, giving a singular continuous spectrum. Below ϵ_c, when the states are extended the dynamics of the classical system is on "three–frequency" quasiperiodic orbits [17] with Lyapunov exponent equal to 0. Above

ϵ_c, localized states correspond to SNAs with negative Lyapunov exponent (see Fig. 2a for an example), while critically localized states at ϵ_c are exceptional and correspond to SNAs with a zero Lyapunov exponent [15]. For energies in the gaps, $\lambda < 0$, and the motion is on two–frequency quasiperiodic (1–dimensional) attractors (an example is shown in Fig. 2b), which wind across the (x, θ) plane an integral number of times. Wavefunctions of Eq. (1) at these energies do not satisfy the appropriate boundary conditions and are non–normalizable. The number of windings of the corresponding attractor, N is a topological invariant for *all* orbits in the gaps. This integer index for each gap [19] counts the number of changes of sign (per unit length) of the wavefunction, and is thus related to the integrated density of states (IDS) [20]. The gap–labelling theorem [20] states that each gap can be labeled by the value that the IDS takes on the gap; in the Harper system, this is also the winding number [19], and (for $E \geq 0$) on the gap labeled by the index N, this takes the value

$$\Omega_N(E) = \max(\{N\omega\}, 1 - \{N\omega\}). \tag{5}$$

(The symmetrically located gap with $E \leq 0$ with index N has winding number $\Omega_N(E) = \min(\{N\omega\}, 1 - \{N\omega\}))$.

There is thus a 1–1 correspondence between the gaps and the integers. Furthermore, since the IDS is a continuous nondecreasing curve, it is possible to specify the gap ordering: this depends on the continued fraction representation of ω. This latter problem has been studied earlier by Slater [21], and is also encountered in the context of level statistics of two–dimensional harmonic oscillator systems [22,23]. Consider the set of numbers $y_j = \{j\omega\}, j = 1, 2, \ldots, m$. For *any* ω and any m, it has been shown [21,22] that an "ordering function" can be defined, giving a permutation of the indices, $j_1, j_2, \ldots, j_m$, such that $y_{j_i} \leq y_{j_k}$ if $i < k$. This result can be directly adapted to the present problem so as to obtain the complete ordering of gap labels with E [24].

The resulting structure of the gaps can be described via a simpler construction for the case of $\omega = \omega_{\rm g}$. Recall that $\omega_{\rm g} = \lim_{k\to\infty} F_{k-1}/F_k$, where the Fibonacci numbers F_k are defined by the recursion $F_{k+1} = F_{k-1} + F_k$, with $F_0 = 1, F_1 = 2$. Now consider a Cayley

tree, arranged as shown in Fig. 3, with each node (except the origin, labeled 0) having two successors. Nodes at the same horizontal level are at the same generation. The rightmost node at each generation is labeled by successive Fibonacci integers, while the leftmost are half the successive even Fibonacci integers. The non–Fibonacci numbers are then identified with nodes as follows: for given label m, the parent node i_m is the smallest available such that the sum $(i_m + m)$ is a Fibonacci number. The sub–tree rooted at node F_k contains a sequence $F_j F_{j+k}, j = 1, \ldots$ which are placed alternately to the left and right; this suffices in determining the placement of all other integers within that subtree [25].

Every pair of integers, i_1 and i_2, with $i_2 > i_1$, has two possibilities as to how they are relatively placed on this graph. Either

1. i_1 is an ancestor of i_2, i.e. there is a directed path connecting i_2 to i_1. If this path is to the left at node i_1, then $i_2 \prec i_1$. (If to the right, then $i_1 \prec i_2$.)

   or

2. i_0 is the most recent common ancestor of i_1 and i_2. If the path from i_0 to i_1 is on the left at i_0, then $i_1 \prec i_2$. (Similarly, if it is to the right, then $i_2 \prec i_1$.)

This gives a unique ordering of the integers (see Fig. 3) with the relation $\prec$ being transitive (if $i \prec j$ and $j \prec m$ then $i \prec m$),

$$\ldots \prec 4 \prec \ldots \prec 9 \prec \ldots \prec 1 \prec \ldots \prec 7 \prec \ldots \prec 2 \prec \ldots \prec 11 \prec \ldots \prec 21 \prec \ldots \prec 0.$$

The gaps appear in *precisely* this order: if $k \prec \ell$, then gap k precedes gap ℓ in the positive energy spectrum of the critical Harper map (Fig. 1b). Following the procedure which is described in detail in [22,23], similar Cayley trees can be constructed for any other irrational frequency. For each ω, depending on its continued fraction representation, there is a unique reordering of the integers corresponding to the ordering of the gaps.

Each gap is further characterized by its width, w_m and by its depth d_m both of which are functions of ϵ. The depth has no obvious quantum–mechanical interpretation, $-d_m$ merely being the minimum value that the Lyapunov exponent takes in the mth gap, and

it decreases with order $d_m > d_n$ if $m < n$, scaling, at ϵ_c as $d_N \sim 1/N$ (see Fig. 4a). The behaviour of the gap widths is more complicated and depends on the details of the Cayley tree. These are nonnmonotonic as a function of gap index, but come in families: gaps belonging to a given family scale as a power, $w_N \sim 1/N^\theta$. The fastest decreasing are the Fibonacci gaps, 1,2,3,5,8,...,F_k,... ($\theta \equiv \theta_r \approx 2.3$), while the slowest is the family 1,4,17,...,$F_{1+3k}/2$,... ($\theta \equiv \theta_l \approx 1.88$): these are respectively the successive rightmost and leftmost nodes on the Cayley tree in Fig. 3 (see Fig. 4b). Other families, which can be similarly defined on subtrees, also obey scaling, with exponents between θ_l and θ_r. When the gaps are ordered by rank r, then they scale as $w_r \sim 1/r^2$: this is consistent with the previously (numerically) obtained [4] gap distribution $\rho(s) \sim s^{-3/2}$, which has also been derived exactly through the Bethe ansatz [26].

Above ϵ_c, the states are exponentially localized. For all localized states, irrespective of energy, the localization length or Lyapunov exponent is identical [5]. The gaps which dominate the spectrum at ϵ_c, persist for larger ϵ, but decrease in width according to the (empirical) scalings (see Fig. 4b)

$$w_N \sim \frac{1}{N^\theta \epsilon^{N-1}} \tag{6}$$

$$d_N \sim \frac{1}{N\epsilon^N}, \tag{7}$$

(where θ is particular to the family to which the gap belongs).

The dynamics of the Harper map corresponding to localized states is on SNAs [14], while that in the gaps continues to be on 1–dimensional attractors similar to those below ϵ_c. However, since the gaps decrease in width, most of the dynamics is now on SNAs. By continuity, therefore, the SNA regions must start at each eigenvalue at ϵ_c, and widen gradually since for large ϵ the spectrum lies in the range $0 \leq E \leq 2\epsilon$. A phase–diagram for this system in the $E - \epsilon$ plane is shown schematically in Fig. 5. The dynamics is entirely on fractal attractors with a negative Lyapunov exponent in the tongue–like regions, each of which starts at an eigenvalue at ϵ_c. The fractal (Cantor set) spectral structure is thus reflected in the hierarchically organized fractal "tongues".

The equivalence between the Harper equation and the Harper map thus provides a new mode of analysis of this problem which arises in numerous contexts [1–9]. The singular continuous nature of the eigenvalue spectrum, which has been the subject of considerable theoretical study, has been detected in experiments [27] as well, and therefore an understanding of the gap widths and their variation with energy and potential strength is of importance.

The present technique gives a simple but powerful method for the study of the spectrum to a finer level of detail than has hitherto been available. As we have demonstrated, in this problem the details are *crucial*: although the spectrum of the Harper equation at ϵ_c is a Cantor set, the gaps may be labeled through a topological invariant of orbits of the Harper map which is related to previously described rotation numbers for such systems [19] and to the integrated density of states [20]. The ordering of the gaps depends on number–theoretic properties of particular irrational frequency ω [21,24], while the gap indices determine the exponents for the scaling of gap widths as a function of potential strength. The phase diagram for the Harper system will consist of fractal tongues for all irrational frequencies ω, and in the tongues, the dynamics of the Harper map is on SNAs. The ubiquity of such attractors and their correspondence with localized states further underscores their importance [14,15].

ACKNOWLEDGMENT: This research is supported by the Department of Science and Technology, India. We have especially benefited from correspondence with Jean Bellisard, and from discussions with Deepak Kumar and Subir Sarkar.

REFERENCES

[1] P. G. Harper, Proc. Phys. Soc. London A **68**, 74 (1955).

[2] D. R. Hofstadter, Phys. Rev. B **14**, 2259 (1976).

[3] See e. g. J. B. Sokoloff, Phys. Rep. **126**, 189 (1985); M. Y. Azbel, P. Bak, and P. M. Chaikin, Phys. Rev. Lett. **59**, 926 (1987); I. I. Satija, Phys. Rev. B **49**, 3391 (1994); H.–J. Stöckmann, *Quantum Chaos, an introduction*, (Cambridge University Press, Cambridge, 1999), Chapter 4; P. B. Wiegmann, Prog. Theor. Phys. Suppl., **134**, 171 (1999); Y. Last, in *XI Intern. Congress of Mathematical Physics (Paris, 1994)*, Ed. D. Iagolnitzer, Intern. Press, Cambridge, MA (1995), pp. 366–372; S. Jitomirskaya, *ibid.*, pp. 373-382.

[4] T. Geisel, R. Ketzmerick, and G. Petschel, Phys. Rev. Lett. **66**, 1651 (1991); also in *Quantum Chaos*, edited by G. Casati and B. Chirikov, (Cambridge University Press, Cambridge, 1995), pp. 633–60.

[5] G. André and S. Aubry, Ann. Isr. Phys. Soc., **3**, 133 (1980).

[6] J. Bellisard, R. Lima, and D. Testard, Comm. Math. Phys. **88**, 107 (1983).

[7] M. Kohmoto, Phys. Rev. Lett. **51**, 1198 (1983); M. Kohmoto, L. P. Kadanoff, and C. Tang, Phys. Rev. Lett. **50**, 1870 (1983)

[8] S. Ostlund, R. Pandit, D. Rand, H. J. Schellnhuber, and E. D. Siggia, Phys. Rev. Lett. **50**, 1873 (1983).

[9] S. Ostlund and R. Pandit, Phys. Rev. B **29**, 1394 (1984).

[10] J. Ketoja and I. I. Satija, Phys. Lett. A **194**, 64 (1994).

[11] J. Ketoja and I. I. Satija, Phys. Rev. Lett. **75**, 2762 (1995).

[12] H. Hiramoto and M. Kohmoto, Int. J. Mod. Phys. **B6**, 281 (1992).

[13] J. -M. Luck, Phys. Rev. B **39**, 5834 (1989).

[14] J. Ketoja and I. I. Satija, Physica D **109**, 70 (1997).

[15] A. Prasad, R. Ramaswamy, I. I. Satija, and N. Shah, Phys. Rev. Lett. **83**, 4530 (1999).

[16] C. Grebogi, E. Ott, S. Pelikan, and J. Yorke, Physica D **13**, 261 (1984); A. Prasad, S. S. Negi, and R. Ramaswamy, Int. J. Bifurcation and Chaos **11**, 291 (2001).

[17] A. Bondeson, E. Ott, and T. M. Antonsen, Phys. Rev. Lett. **55**, 2103 (1985).

[18] For instance, the Hofstadter butterfly [2] can be trivially constructed as the set $\{(E,\omega) : \lambda(E,\omega,\epsilon=1)=0\}$.

[19] The number N of *complete* traversals from $\tanh x = 1$ to $\tanh x = -1$ is related to the winding number defined in R. Johnson and J. Moser, Comm. Math. Phys. **84**, 403 (1982) as $\Omega_N = M + N\omega$, M, N integer. See also F. Delyon and B. Souillard, Comm. Math. Phys. **89**, 415 (1983).

[20] J. Bellisard, in *From Number Theory to Physics*, edited by M. Waldschmidt, P. Moussa, J.-M. Luck, and C. Itzykson, (Springer Verlag, Berlin, 1992), pp. 538–630. J. Bellisard and B. Simon, J. Funct. Anal., **48**, 408 (1982).

[21] N. B. Slater, Proc. Cambridge Philos. Soc. **63**, 1115 (1967).

[22] A. Pandey, O. Bohigas, and M.-J. Giannoni, J. Phys. A **22**, 4083 (1989).

[23] A. Pandey and R. Ramaswamy, Phys. Rev. A **43**, 4237 (1991).

[24] The ordering function, Eq. (6) in [22] or the procedure leading to Eq. (33) in [21] applies to numbers $y_j = \{j\omega\}$ and needs to be slightly modified for application to the present problem where all the Ω_k's are constrained to lie in the interval [1/2,1] since we are considering only positive eigenvalues. The details are unwieldy but not very complicated, and are given in S. S. Negi, Ph D. thesis, Jawaharlal Nehru University, 2001.

[25] Subsidiary number–theoretic properties help in arranging the remaining integers. If m and m' are daughters of i_m, then $(m + i_m)$ and $(m' + i_m)$ are consecutive Fibonacci numbers. Details of the overall scheme will be given in a forthcoming publication.

[26] A. G. Abanov, J. C. Talstra, and P. B. Wiegmann, Nucl. Phys. B **525**, 571 (1998).

[27] C. Albrecht, J. H. Smet, K. von Klitzing, D. Weiss, V. Umansky, and H. Schweizer, Phys. Rev. Lett. **86**, 147 (2001).

FIGURE CAPTIONS

Figure 1: The Integrated density of states (IDS) (scale on the right) and Lyapunov exponent (λ) (scale on the left) versus energy at ϵ_c. The gap labels k are indicated for the largest visible gaps. At every bifurcation, when $\lambda = 0$, the dynamics is on a SNA. On the gaps, the IDS takes the constant value Ω_k specified by Eq. (5).

Figure 2: (a) A strange nonchaotic attractor for ϵ=2, $E = 3$. (b) The attractor for a value of E corresponding to the gap $N = 5$. Note that the orbit has 5 branches that traverse the range $-\infty < x < \infty$.

Figure 3: Ordering of the gaps for ω the golden mean. Only part of the Cayley tree described in the text is shown for clarity. Each node has two daughters except for 0, which has only one.

Figure 4: (a) Scaling of the gap widths, w_N ($\bullet$), and depths d_N ($\diamond$) as a function of gap index, N, at $\epsilon = \epsilon_c$. For clarity, the depths have been multiplied by a factor of 10. The dashed line fitting the depths has slope -1. The dotted lines show the scaling of the two families of gaps; see the text for details. (b) Scaling of the gap widths, w_N for the largest few gaps as a function of ϵ above ϵ_c. The solid lines are the power–laws given in Eq. (6).

Figure 5: Phase diagram for the Harper map showing, below ϵ_c (the dotted vertical line) the regions of three–frequency quasiperiodic (Q) orbits or extended states, 1–d attractors or gaps (G), and above ϵ_c, regions of SNAs (S), and gaps (G). Only the largest gaps are visible at this scale. All the gaps persist above ϵ_c, decreasing in width according to Eq. (6), but the measure of the SNA region (shaded) increases with ϵ, as does the range of the spectrum.

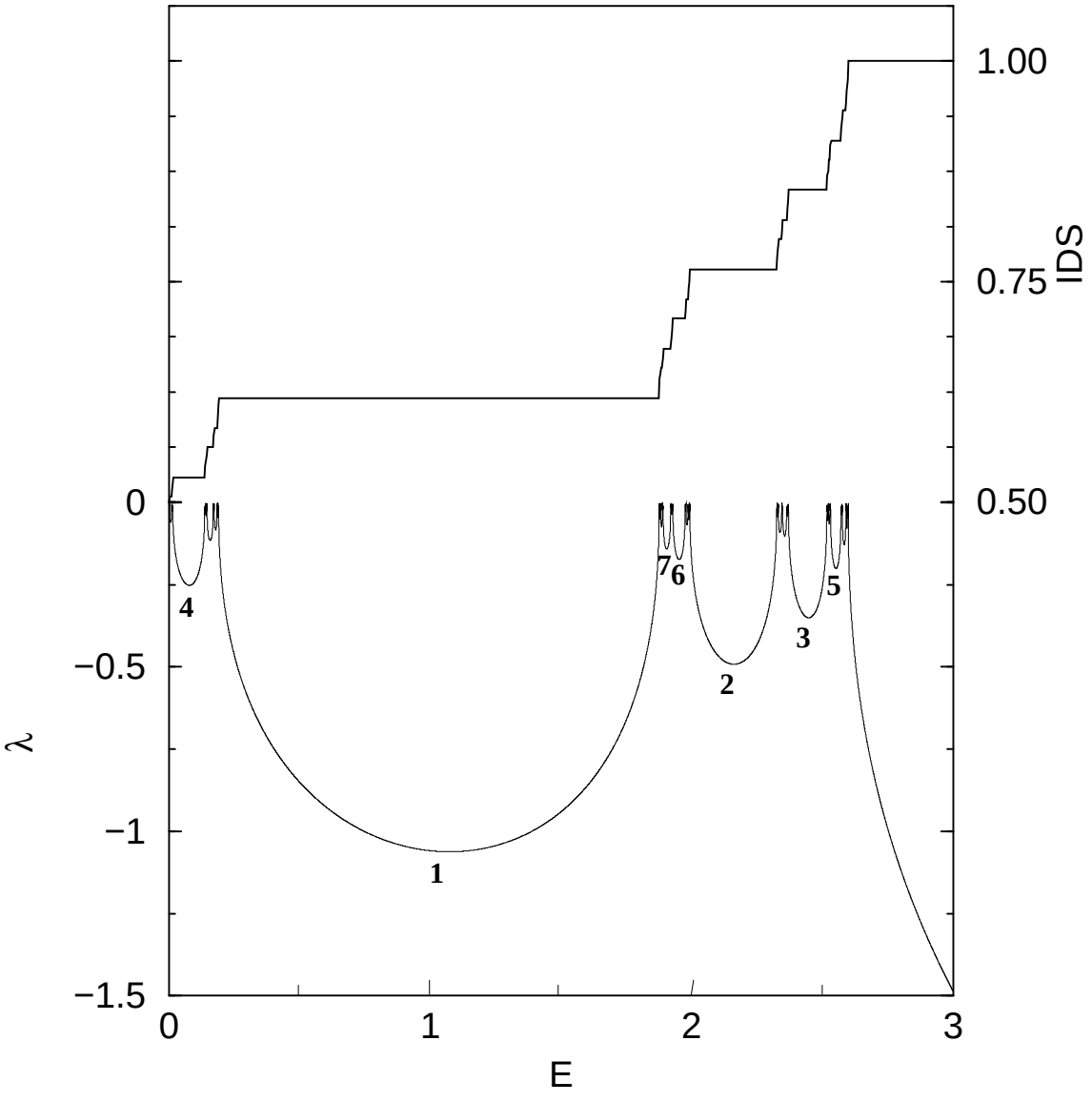
1.00
0.75
0.50
IDS
0
−0.5
−1
−1.5
λ
0
1
2
3
E
1
2
3
4
5
6
7

This figure "fig2.gif" is available in "gif" format from:

http://arXiv.org/ps/nlin/0105013v1

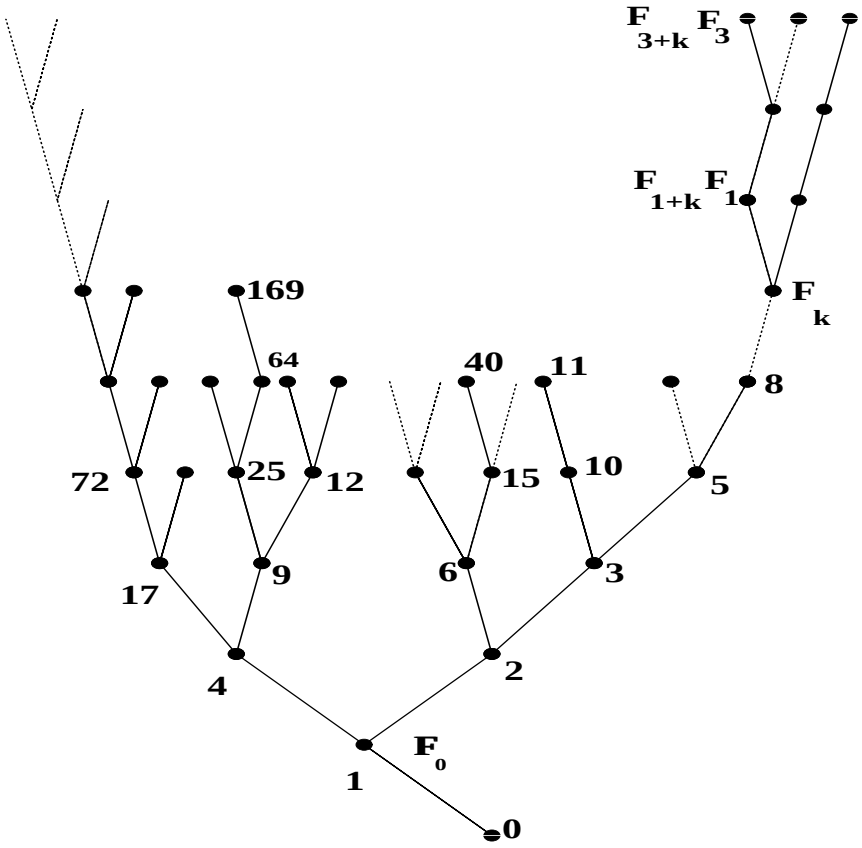
F 3+k
F 3
F 1+k
F 1
F k
169
64
40
11
8
72
25
12
15
10
5
17
9
6
3
4
2
F 0
1
0

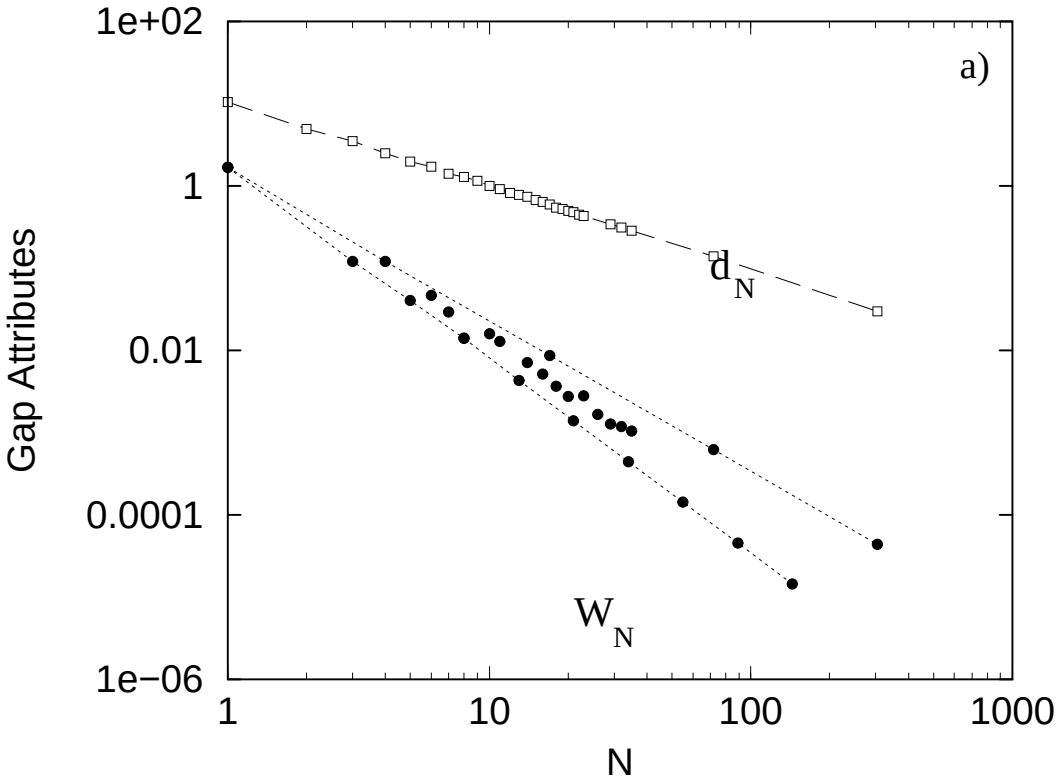
a)
1e+02
1
0.01
0.0001
1e−06
Gap Attributes
1
10
100
1000
N
d_N
W_N

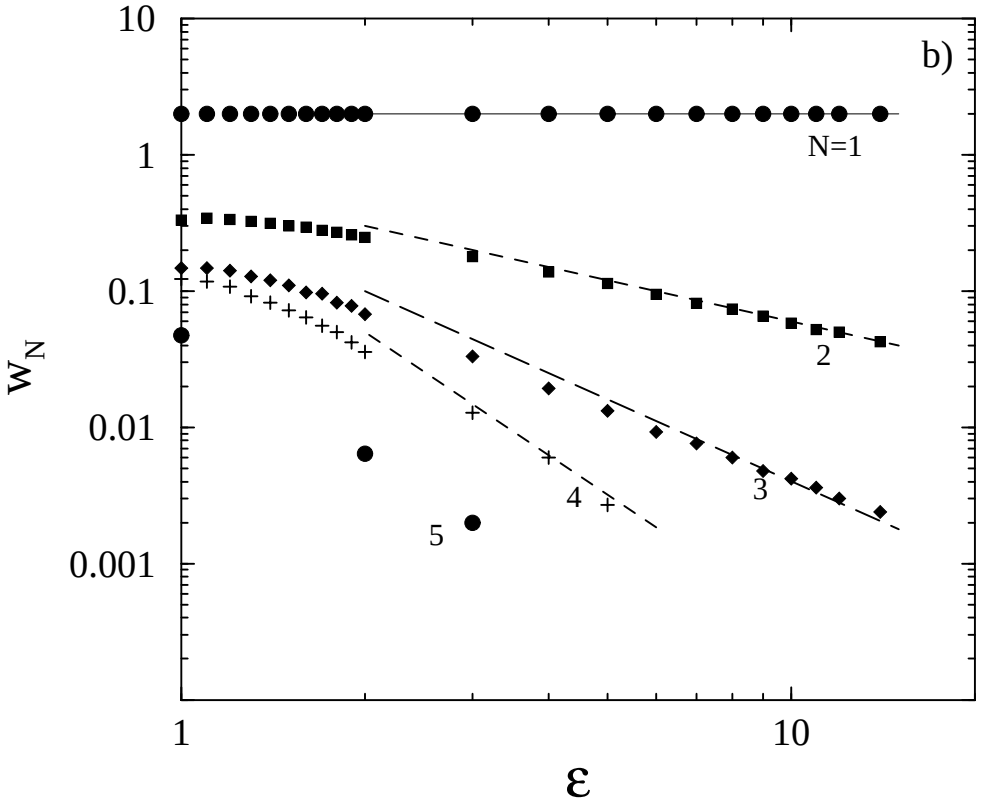
b)
10
1
0.1
0.01
0.001
W_N
1
10
ε
N=1
2
3
4
5

This figure "fig5.gif" is available in "gif" format from:

http://arXiv.org/ps/nlin/0105013v1